Universitat Politècnica de Catalunya (UPC)

Role of the residual layer and large–scale subsidence on the development and evolution of the convective boundary layer

Estel Blay–Carreras, **David Pino**, Jordi Vilà–Guerau de Arellano, Anneke Van de Boer, Olivier Decoster, Oscar Hartogensis, Henk Pietersen, Marie Lothon, Clara Darbieu, Fabienne Lohou

Motivation

- Which role play RL during the morning transition?
- How important is subsidence during the whole evolution of the convective boundary layer?
- How potential temperature, boundary–layer depth and TKE budget evolve depending on the presence of RL?
- What are the consequences to the observed CO_2 mixing ratio?

Methodologies

- Observations taken during the BLLAST campaign (1st July, IOP9). Eddy Covariance instruments at SS1 and radioundings.
- Large-Eddy Simulations (DALES, Heus et al., 2011). Sensitivity studies varying the initial profile and subsidence.
- Mixed-layer model. Subsidence is taken into account.

Numerical experiments

DALES (Heus et al., 2011)
256^3 points. 12.8x12.8x3 km^3 domain
From 0730 until 2000 UTC.
MLM from 1100 UTC (developped CBL). Includes subsidence
Surface Flux mean of EC observations at SS1

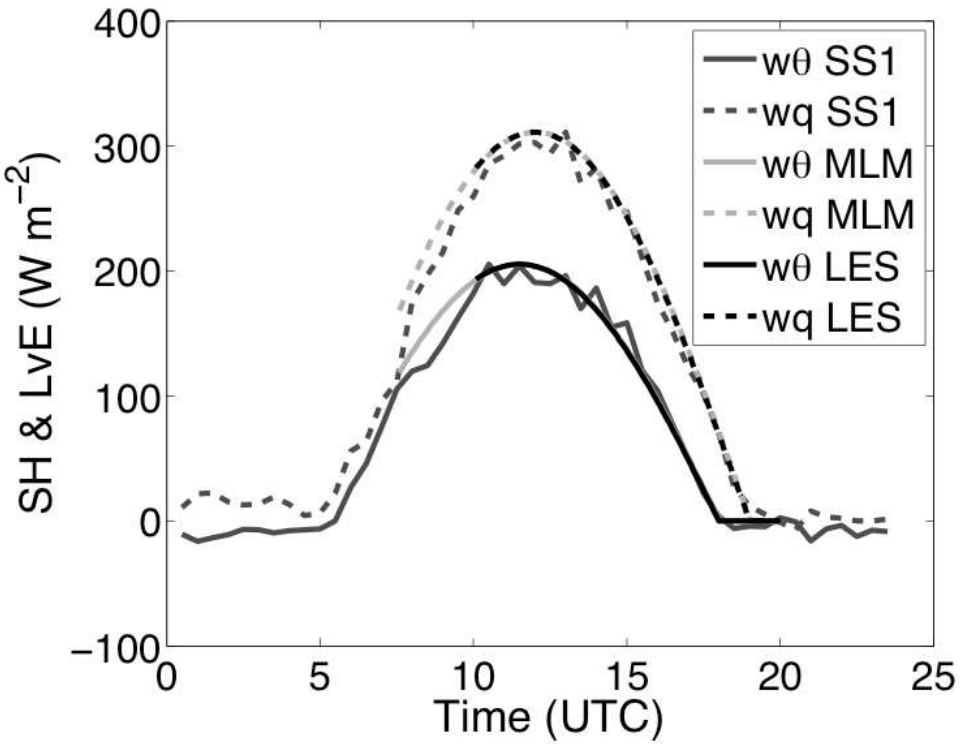

Numerical experiments

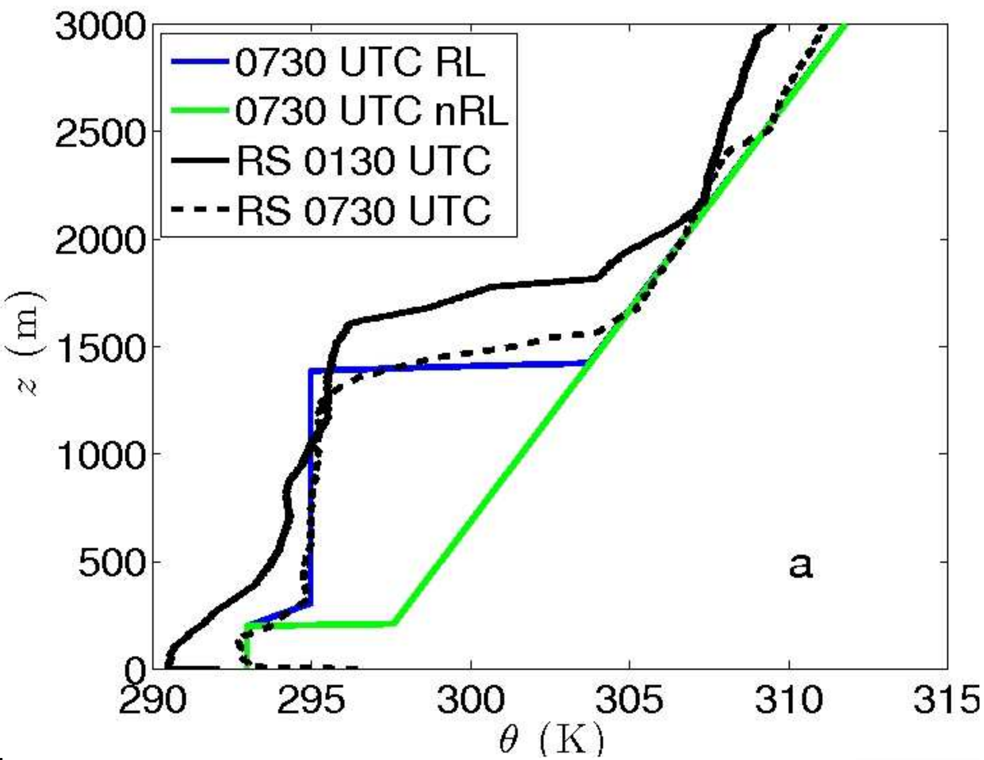

DALES (RL) initial profile based on radiosoundaing at 0730 UTC.
Same FA lapse rate

Subsidence calculated by comparing 0130 and 0730 UTC soundings (215 m in 6 h)
Subsidence velocity → 9.95 · 10^{-3} m s^{-1}

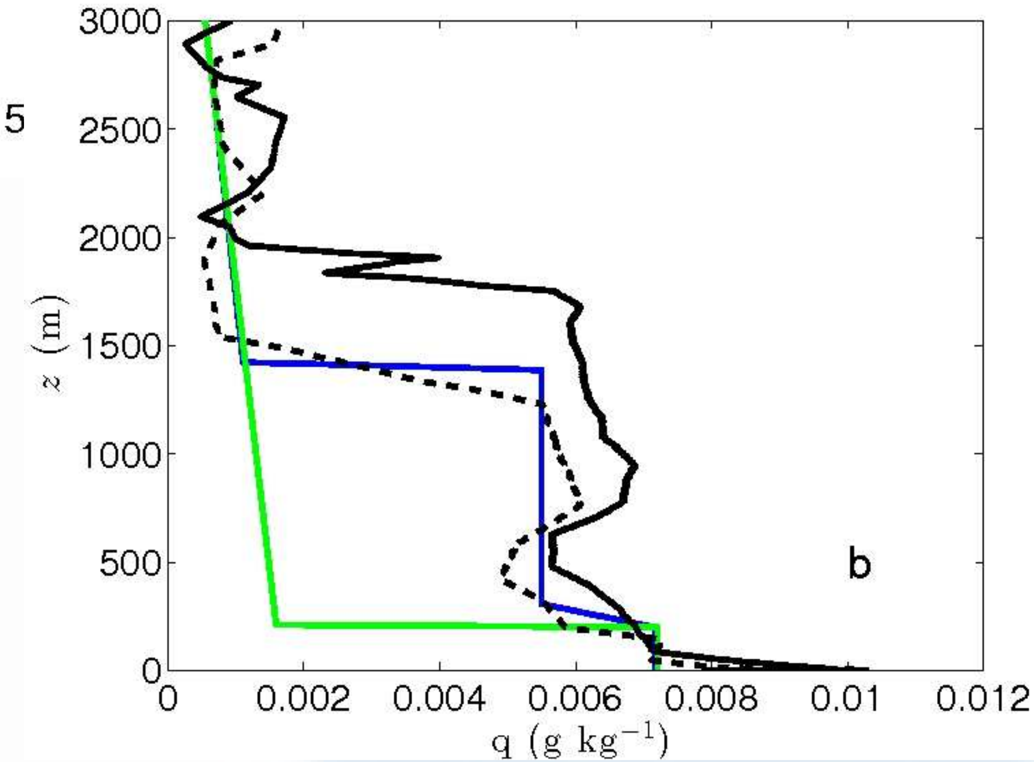

Universitat Politècnica de Catalunya (UPC)

Numerical experiments

Initial wind profile (based on RS at 0730 UTC)

- below the FA → u = −2.95, v = 0.52 m s^{-1}
- At FA similar to geostrophic wind

Geostrophic wind: u_g= 10, v_g= 0 m s^{-1} → constant with height

Four different DALES runs are performed by combining residual layer & subsidence

	0730 UTC		1100 UTC
	RL	nRL	MLM
$\theta_{1,0}$ (K)	293	293	295.5
$\Delta\theta_{1,0}$ (K)	2	5	8
$z_{1,0}$ (m)	210	210	1300
$\theta_{RL,0}$ (K)	295	-	-
$\Delta\theta_{RL,0}$ (K)	9	-	-
$z_{RL,0}$ (m)	1422	-	-
γ_θ (K m^{-1})	0.005	0.005	0.005
$q_{1,0}$ (g kg^{-1})	7.16	7.16	8
$\Delta q_{1,0}$ (g kg^{-1})	-1.66	-5.66	-5
$q_{RL,0}$ (g kg^{-1})	5.50	-	-
$\Delta q_{RL,0}$ (g kg^{-1})	4.41	-	-
γ_q (g (kg m)$^{-1}$)	-0.00035	-0.00035	-0.00035

Results

Temporal evolution of:

- Potential temperature vertical profile
- 2-m potential temperature
- Boundary layer depth (first inversion from the surface)
- Turbulent kinetic energy vertical profile

- Observations CO_2 mixing ratio & surface flux

Potential temperature vertical profile

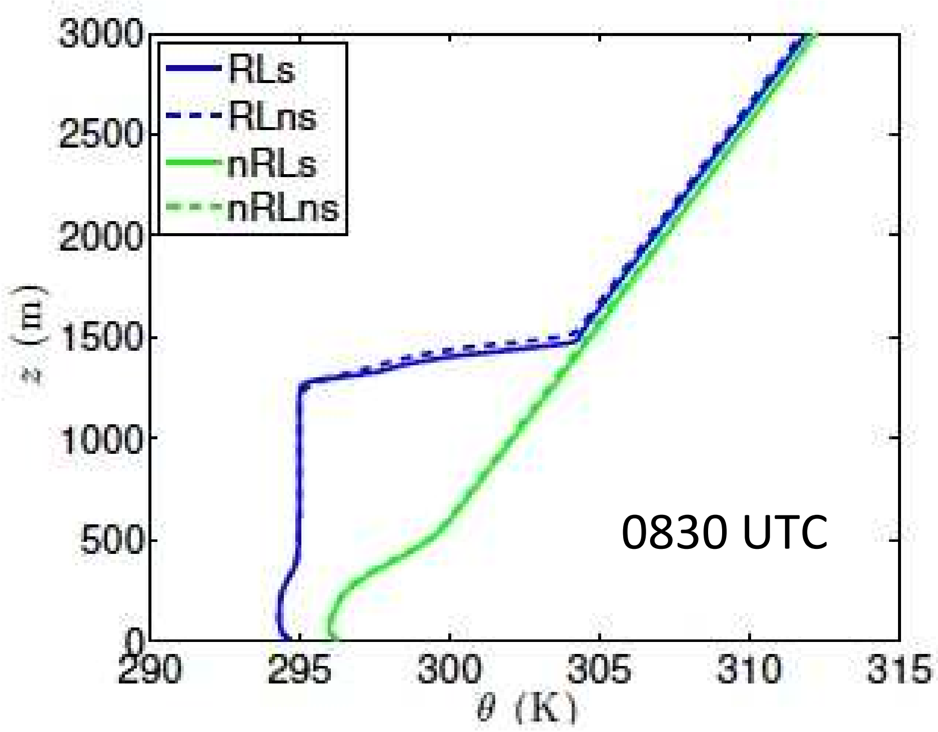

RLs case (solid blue) fit the potential temperature measured by RS

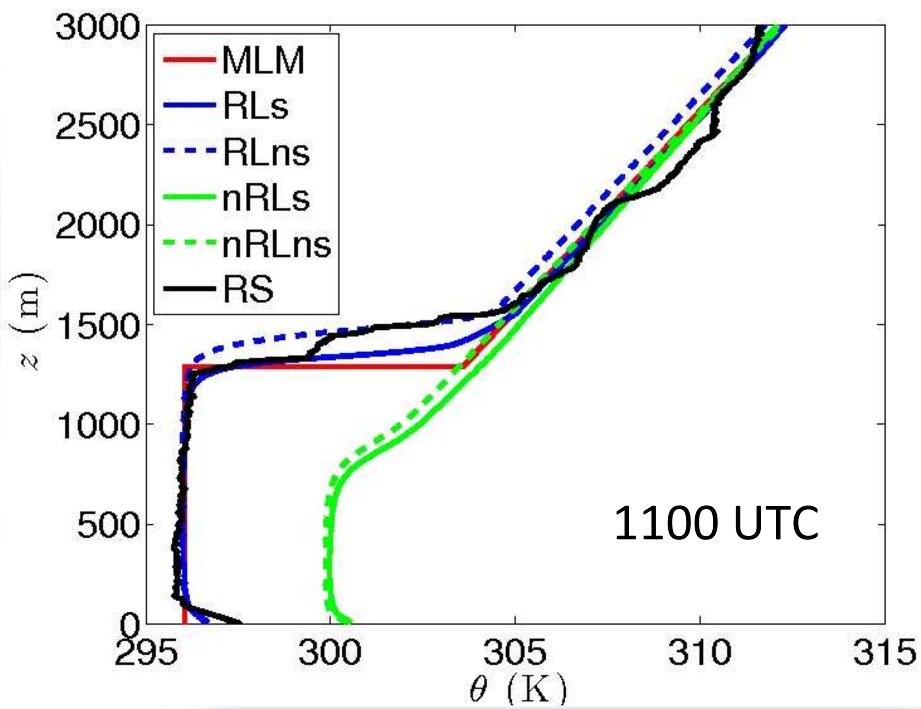

Potential temperature vertical profile

RLs case (solid blue) fit the potential temperature measured by RS

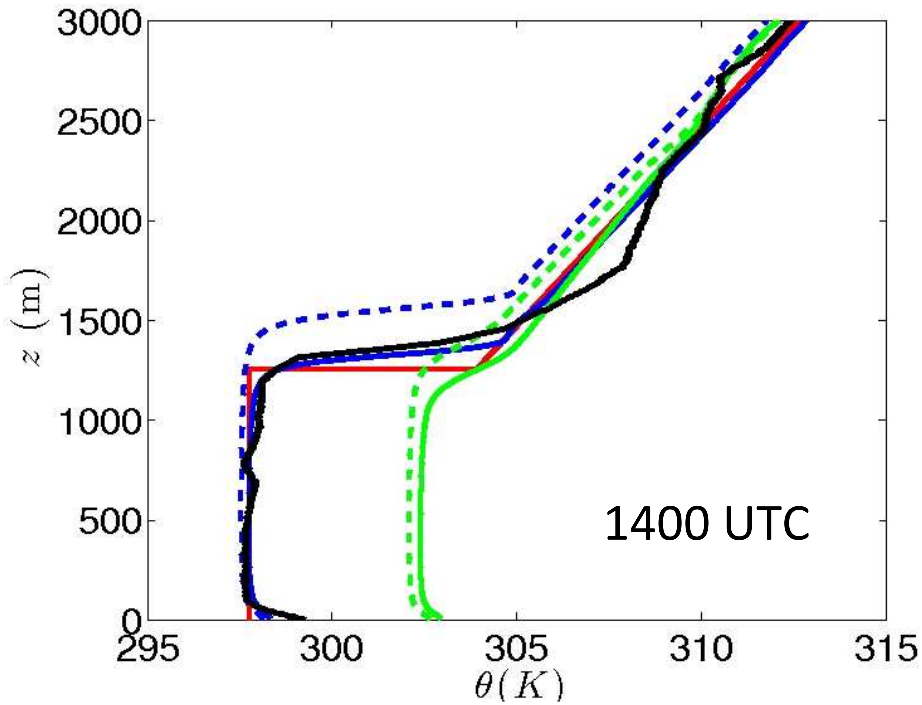

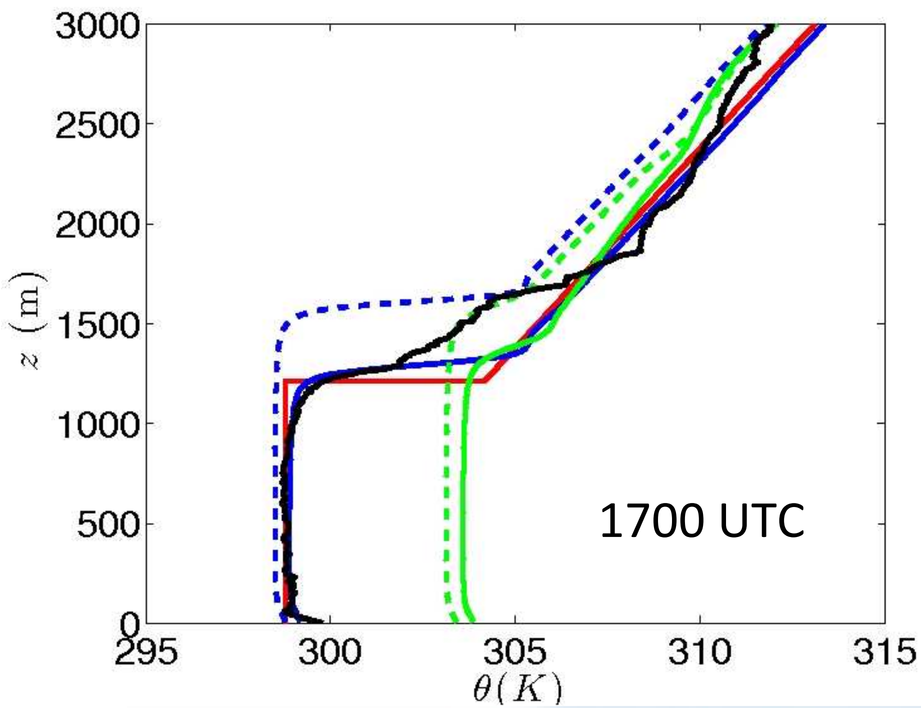

Mixed–layer potential temperature

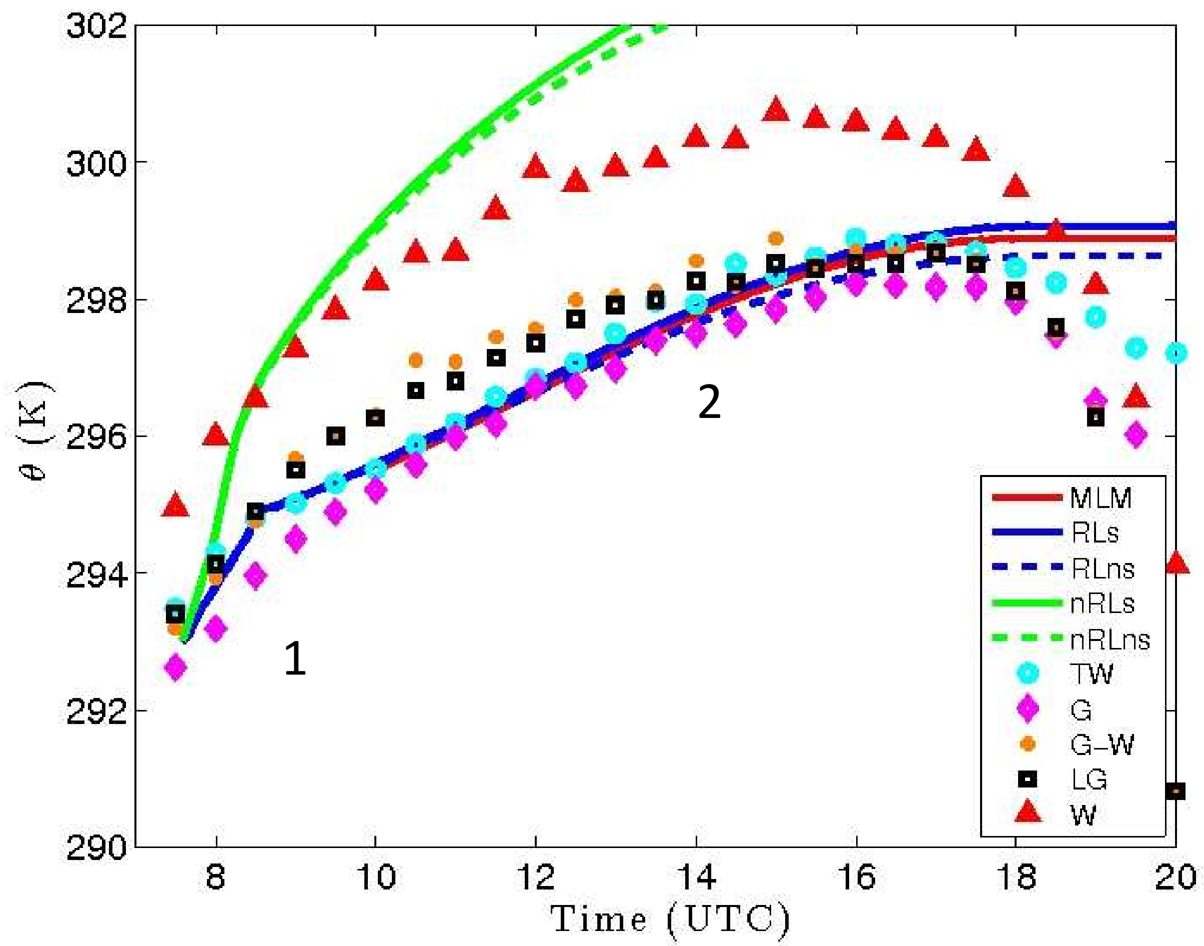

Larger heat fluxes observed over wheat (Nadeau et al., 2011)

Two regims observed (symbols):

1. Low BL, large inversion. Large heating rate.
2. Large BL, smaller inversion. Smaller heating rate.

Mixed–layer potential temperature

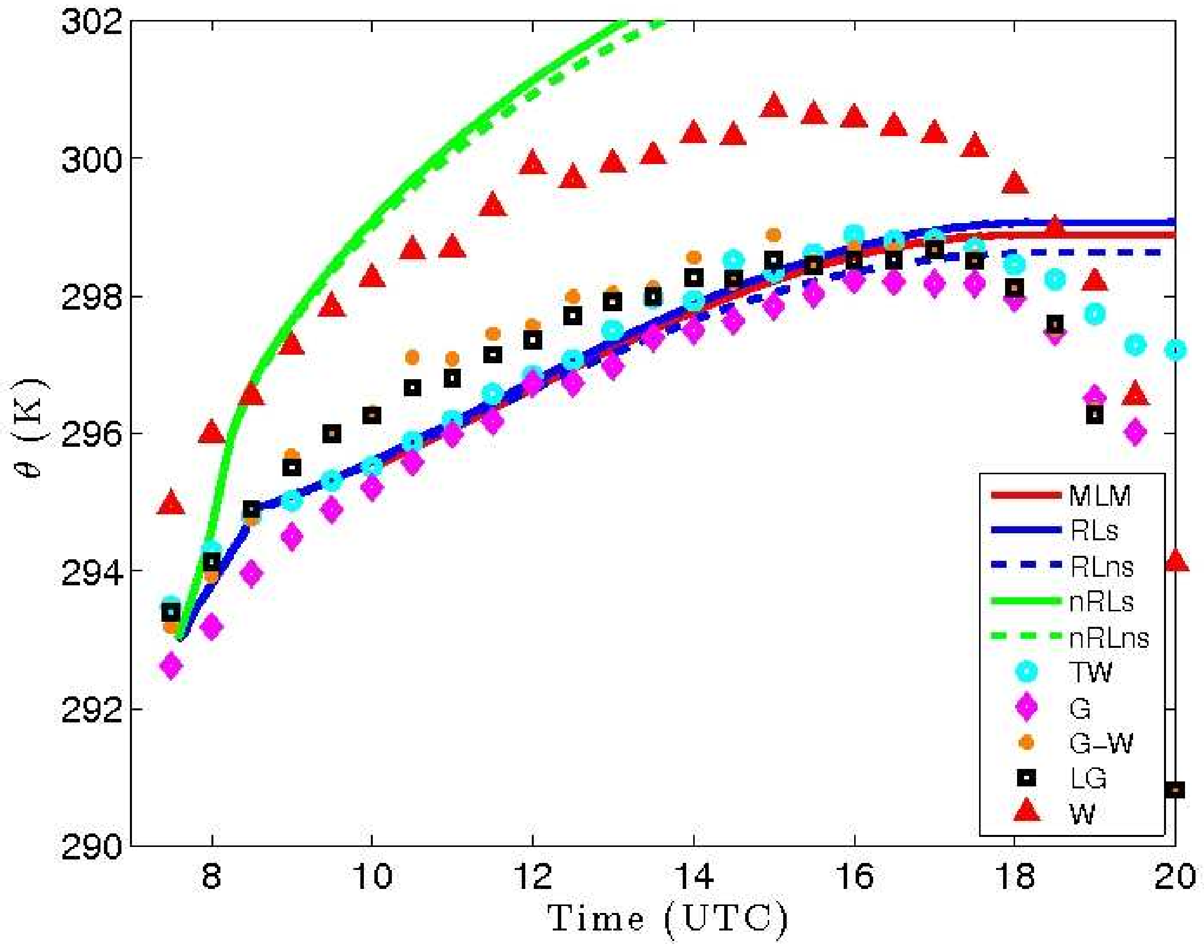

Same surface heat flux for all numerical experiments (lines).

RL (blue) cases fit observations. Two regimes are simulated.
nRL (green) overestimates the observed 2-m temperature.

Boundary–layer depth temporal evolution

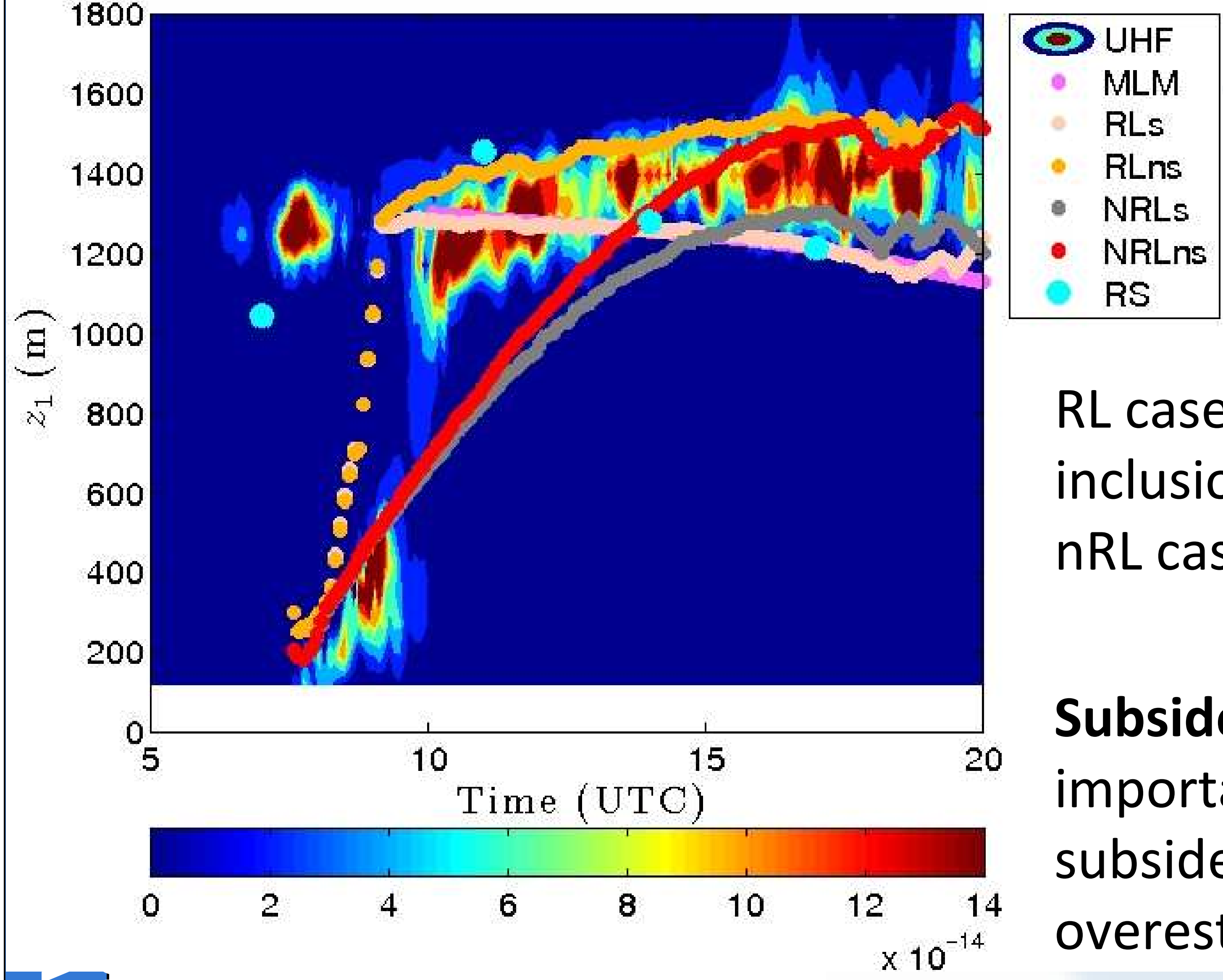

Minimum buoyancy flux

Maximum virtual potential temperature gradient

RL cases simulate the inclusion of RL into BL

nRL cases → 4 hours delay

Subsidence play an important role → no subsidence cases overestimate the depth 200 m

Entraiment heat flux

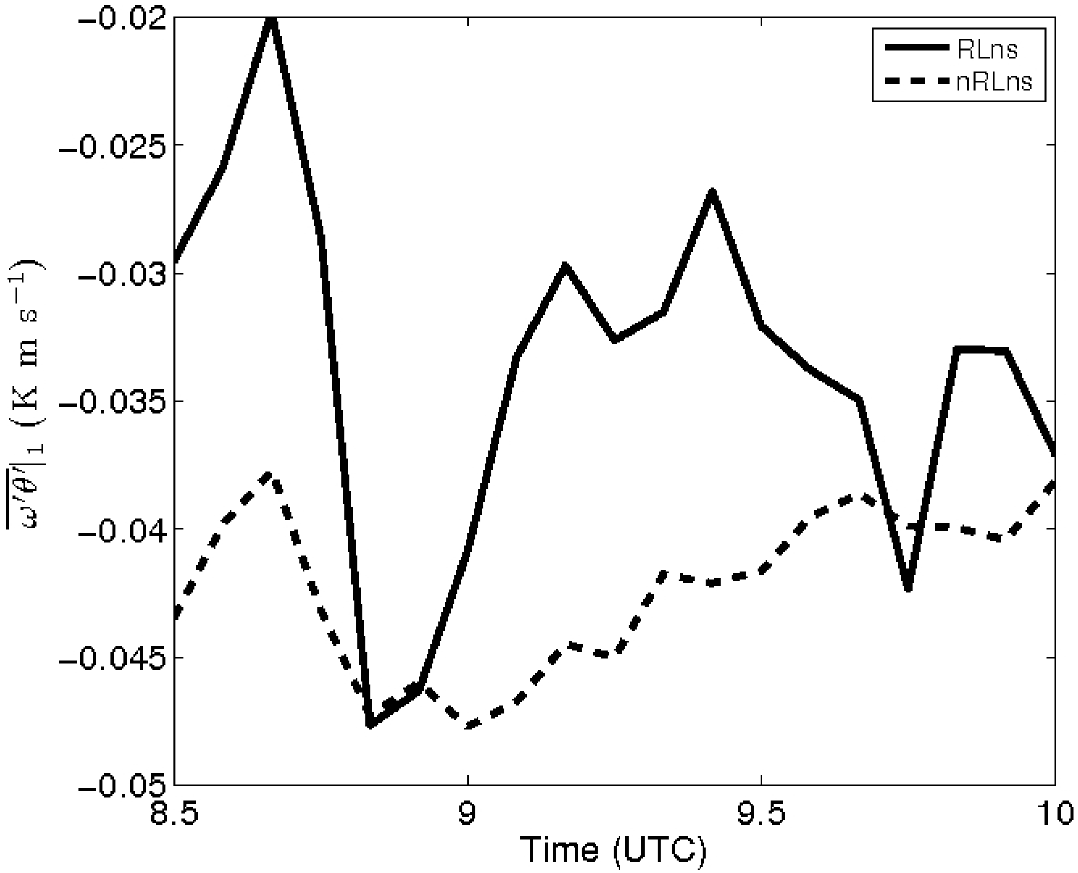

Before the transition larger entrainment fluxes for the nRL case (strong inversion).

At the transition, the minimum of the heat flux increases due to the increase of $\Delta\theta_1$ and entrainment velocity.

Afterwards, RL and nRL cases present similar entrainment flux.

Turbulent kinetic energy budget

$$\frac{\partial \bar{e}}{\partial t} = -\left[\overline{u'w'}\frac{\partial u}{\partial z} + \overline{v'w'}\frac{\partial u}{\partial z}\right] + \frac{g}{\theta_{vr}}\overline{w'\theta'_v} - \frac{\partial \overline{w'e}}{\partial z} - \frac{1}{\rho_0}\frac{\partial \overline{w'p'}}{\partial z} - \varepsilon$$

Larger Shear and Buoyancy terms for nRL during the early morning (Beare, 2008)

Turbulence decreases when BL grows and inversion weakens

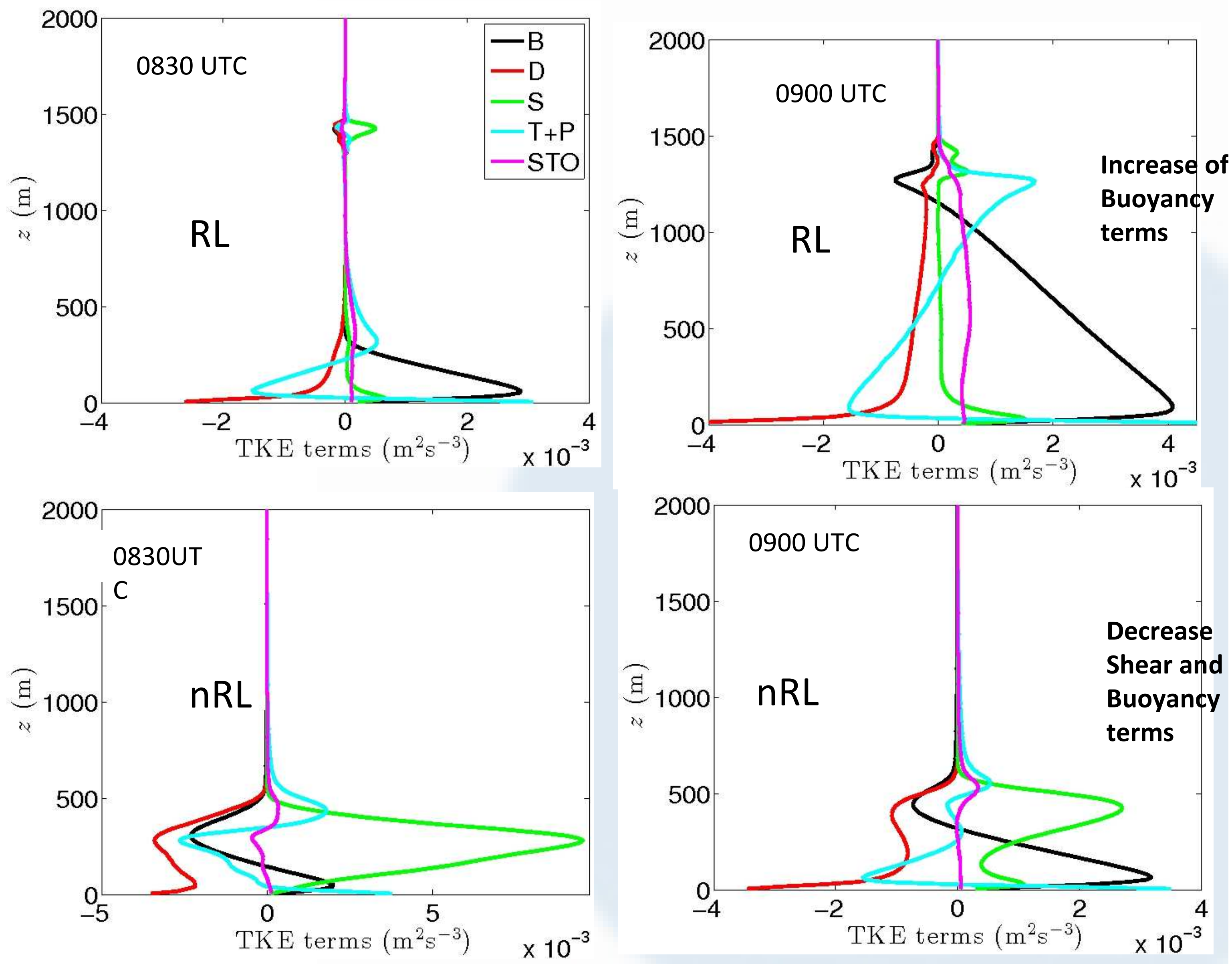

Universitat Politècnica de Catalunya
UPC

Conclusions

- **DALES RL** cases fit the observations.
- During the inclusion of RL, entrainment heat flux increases. Afterwards, similar entrainment heta flux is obtained for all the cases.
- Subsidence is important to correctly simulat the BL-evolution during the afternoon.
- **Shear** and **buoyancy** terms are the **largest during morning**. After the inclusion of the RL, buoyancy increases in the lower part of the CBL and at the inversion and shear decreases at the inversion.

Universitat Politècnica de Catalunya (UPC)

CO_2 surface flux and mixing ratio

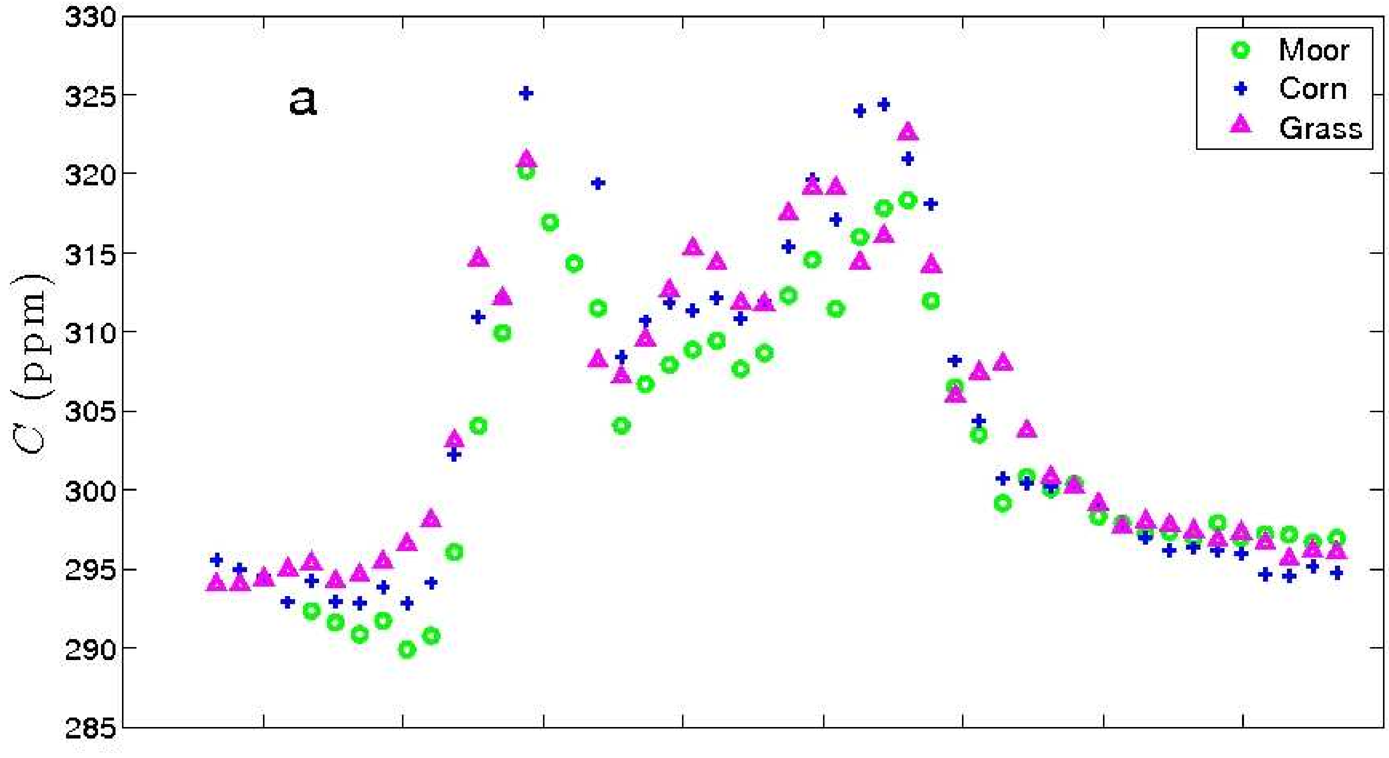

0600 – 0900 UTC → important **decrease** of the CO_2 mixing ratio due to entrainment.

Transition cannot be observed in the CO_2 mixing ratio

For all the land uses, C is approx constant (less than 1 ppm variation) from midday.

Universitat Politècnica de Catalunya

CO_2 surface flux and mixing ratio

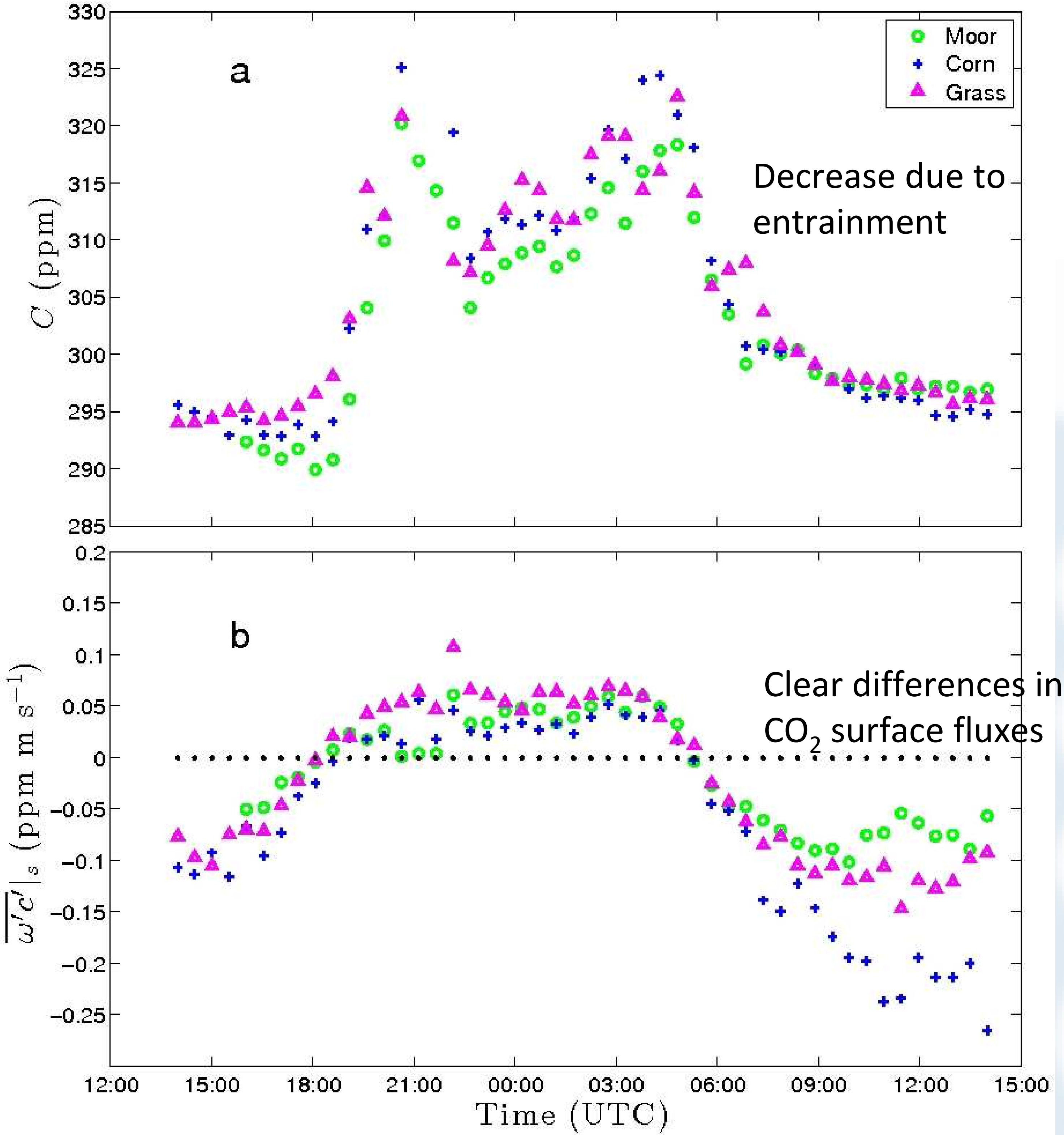

Decrease due to entrainment

Clear differences in the CO_2 surface fluxes

Universitat Politècnica de Catalunya (UPC)

Conclusions

- During the morning, **CO_2 mixing ratio decreases** even with positive CO_2 fluxes due to the importance of CO_2 entrainment flux.

- During the afternoon, **CO_2 mixing ratio** is almost **constant** and small differences are found depending on the landuse (storage term is very small) due to the large value of z_1.